Desalination and Water Treatment
www.deswater.com

doi: 10.5004/dwt.2022.28500

262 (2022) 290–297
June

Effects of mixing conditions on floc breakage and re-growth formed by magnesium hydroxide and polyacrylamide

Jianhai Zhao[a,*], Anmin Wang[a], Linling Mei[a], Wenqi Ge[b], Wenpu Li[a], Hongying Yuan[a]

[a]*Tianjin Key Laboratory of Aquatic Science and Technology, School of Environmental and Municipal Engineering, Tianjin Chengjian University, Tianjin 300384, China, Tel. +8622-23085117; Fax. +8622-23085555; emails: jhzhao@tcu.edu.cn (J. Zhao), 550902426@qq.com (A. Wang), 240410158@qq.com (L. Mei), hitlwp@126.com (W. Li), yuanhy_00@163.com (H. Yuan)*
[b]*School of Control and Mechanical Engineering, Tianjin Chengjian University, Tianjin 300384, China, Tel. +8622-23085136; email: gewenqi@tcu.edu.cn*

Received 1 November 2021; Accepted 12 April 2022

ABSTRACT

Polyacrylamide (PAM) compounding with magnesium hydroxide as dual-coagulant for treating reactive orange simulated wastewater was studied in this paper. Effects of mixing conditions on floc properties, breakage and re-growth were evaluated through floc size distribution, zeta potential, scanning electron microscopy and Fourier-transform infrared spectroscopy. The aggregation and breakup of flocs showed that there was an increase of floc size and strength under proper shear. When floc size reached to 62.30 μm at slow mixing period, then breakage at 300 rpm for 60 s, at next slow period at 60 rpm for 3 min, the floc size increased to 78.75 μm. Flocs re-grew rapidly after breakage and sedimentation time was reduced to 40 s. All of the flocs under investigation showed a strong capacity to re-growth when they had been previously broken. During dual-coagulant system, adsorption of magnesium hydroxide and bringing function of PAM were the mainly coagulation mechanisms for reactive orange K-GN removal.

Keywords: Magnesium hydroxide; Polyacrylamide; Reactive orange; Breakage; Re-growth

1. Introduction

In reactive dyes wastewater treatment process, magnesium hydroxide has been proved to be a cheap, environmentally friendly and effective coagulant [1–5]. The mechanisms of magnesium hydroxide for color removal were charge neutralization, precipitate enmeshment and adsorption [6–8]. Flocs formed fast by magnesium hydroxide in rapid mixing period, then grew slowly in flocculation and sedimentation stages. The flocs are still relatively small and coagulation process needs longer sedimentation time to settle down [8,9]. Polyacrylamide (PAM) are commonly used as coagulant aid in wastewater treatment process to improve flocculation [10–12]. PAM can create bridges between destabilized particles, forming large aggregates with good settling properties [13]. Floc size distribution (FSD), breakage, re-growth and settling characteristics are the main parameters influencing pollutants removal in a real wastewater treatment unit [14]. Large flocs and short operation time are important for good performance in coagulation process. Floc breakage should be avoided as far as possible in the coagulation process, but in practice, there exists a high shear force region, which will inevitably break the agglomeration flocs [15,16].

Several authors have found that mixing conditions influenced the coagulation process and flocs properties [15,17,18]. They indicate that high mixing speed will break the flocs, and only part of the flocs will aggregate again after the flocs are broken. It is inevitable for flocs breakage and re-growth, and the effects of shear force on floc

* Corresponding author.

formation, break-up and re-aggregation are related to coagulant type and mechanisms of coagulation.

Although there are some studies on breakage and re-growth using conventional coagulants such as aluminum, iron and magnesium salts, there have been limited studies on magnesium hydroxide coupling with PAM flocculation in reactive dyes system. The main objective of this laboratory study was to evaluate floc breakage and re-growth by magnesium hydroxide and PAM dual-coagulant, especially to understand the effects of breakage time, strength and re-growth time on floc breakage and aggregation.

2. Materials and methods

2.1. Synthetic test water and coagulant

The simulated reactive dye wastewater samples were prepared by adding reactive orange K-GN (Jinan Haoxing Chemical Engineering Co., China) into deionized water to provide concentration of 0.25 g/L. NaOH solution was added to wastewater sample to control initial pH value of 12. A pH-meter (PH_S-25 Shanghai Jinke industrial Co., China) was used to determine the pH of the solutions. $MgCl_2{\cdot}6H_2O$ (CP. Tianjin Chemical Reagent Co., China) was used to prepare magnesium hydroxide coagulant. Magnesium ion was analyzed with an ICS-1500 (Dionex, USA) ion chromatography system. Non-ionic PAM (CP. Tianjin Chemical Reagent Co., China) was used as coagulant aid in coagulation process. K-GN concentration after coagulation process was analyzed by UV-Visible spectrophotometer (UV2550 Shimadzu, Japan) with maximum absorbance wavelength 476 nm. Removal efficiency of reactive dye can be calculated from the concentration changes.

2.2. Jar test procedures

Batch coagulation experiments were carried out on a program controlled jar-test apparatus with 1-L beakers (ZR4-6, Zhongrun Water Industry Technology Development Co., China) at 20°C ± 1°C. The solutions were stirred rapidly at 250 rpm for 90 s during 100 mg/L magnesium ion addition, then 6mg/L PAM was added as coagulant aid, followed by stirring at 60 rpm for 3 min and settled for 5 min before finial concentration of reactive orange was measured. To gain further insight into the floc breakage and re-growth, additional experiments of coagulation process were investigated. After slow mixing at 60 rpm for 3 min, flocs were broken again at breaking mixing speed (200–400 rpm) for 30–120 s, and then re-growth mixing speed (40–90 rpm) for 1–5 min for the flocs to re-grow. During coagulation periods, an on-line intelligent Particle Dispersion Analyzer (iPDA) was used to monitor flocculation index (FI). A schematic diagram of the experimental process is shown in Fig. 1.

2.3. Floc size distribution and properties analysis

Floc size distribution (FSD) was measured before sedimentation by Mastersizer 2000 (Malvern, UK) and each sample was measured three times and obtained the average results. Suspensions were taken from the jar test experiment for zeta potential determination by Zetasizer Nano ZS (Malvern, UK). After sedimentation finished, flocs and sediments were withdrawn from the bottom of the mixture and filtered through filter paper, then natural drying for properties analysis. Floc image was captured by IX71 digital photomicrography (Olympus, Japan). Crystallinity of the sediments was determined by X-ray diffraction (XRD) with CuKα radiation (D/MAX-Ultima IV, Japan). Morphology and properties were analyzed by scanning electron microscopy (SEM FEI, Quanta 200, Czech) and by infrared spectrum analysis (Nicolet iS 10 FT-IR Spectrometer, Thermo Scientific, USA).

3. Results and discussion

3.1. Coagulation performance under different operations

Jar test experiments were performed to investigate the effects of breakage on coagulation performance and floc properties. Two operations were carried out including: (1) the solutions were stirred rapidly at 250 rpm for 90 s, followed by stirring at 60 rpm for 5 min and settled before finial removal efficiency was measured. (2) the solutions were also stirred rapidly at 250 rpm for 90 s, followed by stirring at 60 rpm for 3 min and settled 1 min then broken at 250 rpm 30 s, stirred slowly again at 60 rpm for 3 min and settled. According to FI value, floc size significantly increased when PAM addition at 90 s. As shown in Fig. 2a, FI values were relatively stable under slow mixing conditions without breakage. Flocs settled down for 1 min and FI values reduced quickly because of few flocs suspending in the solution. When flocs were broken at 330–360 s, almost all flocs returned to solution, FI values increased significantly although they were relatively smaller than that of in early slow mixing period. Through re-growth at second slow mixing period, FI values are relatively larger than that of normal coagulation process without breakage. This is different from other findings that a limited capacity to re-growth when they had been previously broken [18,19].

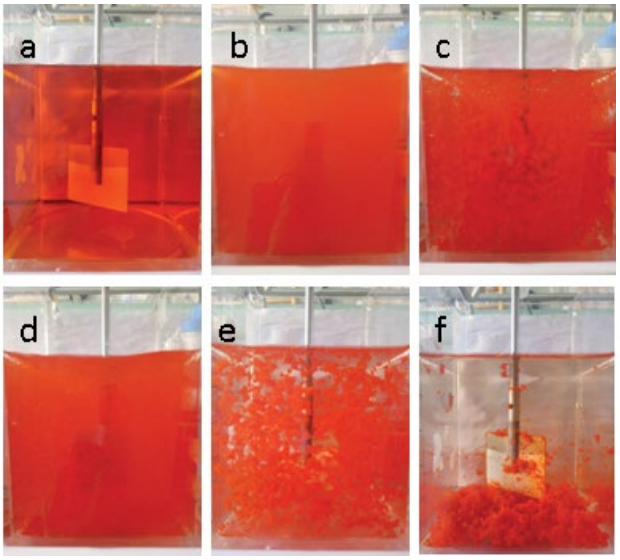

Fig. 1. Coagulation–flocculation process in different stages (a) raw solutions, (b) rapid mixing, (c) slow mixing, (d) breakage, (e) re-growth, and (f) sedimentation.

After breakage and re-growth, the flocs reach their steady-state size during sedimentation process. Fig. 2b shows the reactive dye removal efficiency and settling performance of flocs with and without breakage. Two operations had the same removal efficiency of 99.3% but the settling time was different. This removal efficiency is higher than the findings of our previous studies [8,9]. Because of PAM addition, the settling time reduced from 60 to 40 s through breakage and re-growth. The results show that large floc size leads to higher FI and have good settlement properties.

3.2. Effects of breakage and re-growth on FSD

3.2.1. Effect of breakage on FSD

FI values suggested flocs changes rather than real floc size distribution in coagulation process. In order to obtain real floc size of magnesium hydroxide and PAM dual coagulant for reactive orange removal with and without breakage, FSD was measured after re-growth period. Jar test experiments were performed to investigate the effects of breaking speed and time on FSD after flocs formation and growth. Break-up speed was chosen 200, 300 and 400 rpm and breaking time was 30, 60 and 120 s after normal slow mixing finished. The re-growth time and speed were fixed at 3 min and 60 rpm. Fig. 3 shows the effects of breaking conditions on FSD. As shown in Fig. 3A, the median size of flocs increased as the breakage time increased from 30 to 120 s, and all the flocs through breakage and re-growth were larger than that of normal coagulation without breakage. Fig. 3a also shows cumulative data of floc size. D10, D50 and D90 represent the particle diameter corresponding to 10%, 50%, 90% cumulative undersize particle size distribution, respectively. D50 is also called average floc size or median diameter. D50 increased from breaking time 0 (without breakage) to 60 s and then remained stable in 120 s. Fig. 3B and 3b show the same trends and the highest average floc size was 78.7 μm when breaking speed was 300 rpm. When breaking speed increased from 300 to 400 rpm, significant drops in D10, D50 and D90, as a result of floc breakage, can be observed immediately when shear rate is increased. This is consistent with the findings of previously study [19,20]. Zhan et al. [21] evaluated the influence of velocity gradient (G) on floc property and found that the G values in mixing phase had greater influence on the flocs. When G value is low, increasing G value can increase floc size. Under the condition of medium intensity G value, the flocculation rate reaches the maximum and the floc with the maximum particle size can be obtained. In the case of high G value, floc breakage is dominant. The relationship between sheer strength and G value in the experiment is shown in Table 1.

Combined with the experimental results, it was found that under the condition of relatively lower G value, the floc could not be fully broken, thus affecting its re-growth ability. However, the relatively high G value will hinder the regeneration ability of broken floc. Therefore, the best G value selected in this experiment is 161.5 s^{-1} with the breaking speed 300 rpm.

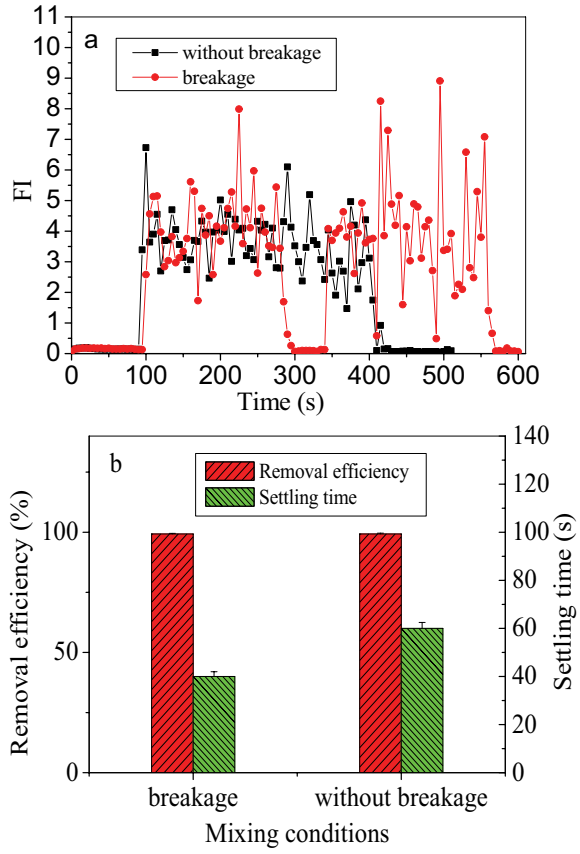

Fig. 2. Coagulation performances with and without breakage (a) FI values with time and (b) removal efficiency and setting time.

3.2.2. Effect of re-growth on FSD

To gain further insight into the floc breakage and re-growth after breaking conditions, additional effects of re-growth time and speed on FSD were investigated. The stirring was set at 250 rpm for 90 s, then slow mixing at 60 rpm for 3 min, 300 rpm for 60 s to break the flocs and then re-grow. The re-growth conditions were as follows: re-growth time from 1 to 5 min for 60 rpm and re-growth speed from 40 to 90 rpm for 3 min. As shown in Fig. 4A and 4a, the average floc size increased as re-growth time increased from 1 min to 3 min, prolonged re-growth time gave relatively small floc size. Fig. 4B and 4b also show that the trends of floc size increased with re-growth speed from 40 to 60 rpm. When increasing re-growth speed to 90 rpm, average floc size decreased again. Colomer et al. [22] investigated the aggregation and breakup of particle flocs under low-shear flow and found that there was an increase of floc size at increasing G values. Re-growth speed 60 rpm (G = 18.5 s^{-1}) was the most suitable strength for flocs aggregation (Table 2).

3.3. Cumulative data of FSD and zeta potential

The optimal conditions were obtained through experimental exploration as follows: rapid mixing 250 rpm for 90 s, followed by slow stirring at 60 rpm for 3 min and then broken at 300 rpm 60 s, stirred slowly again at 60 rpm for 3 min and settled, cumulative data of FSD during each stage in the whole process were measured by laser particle size

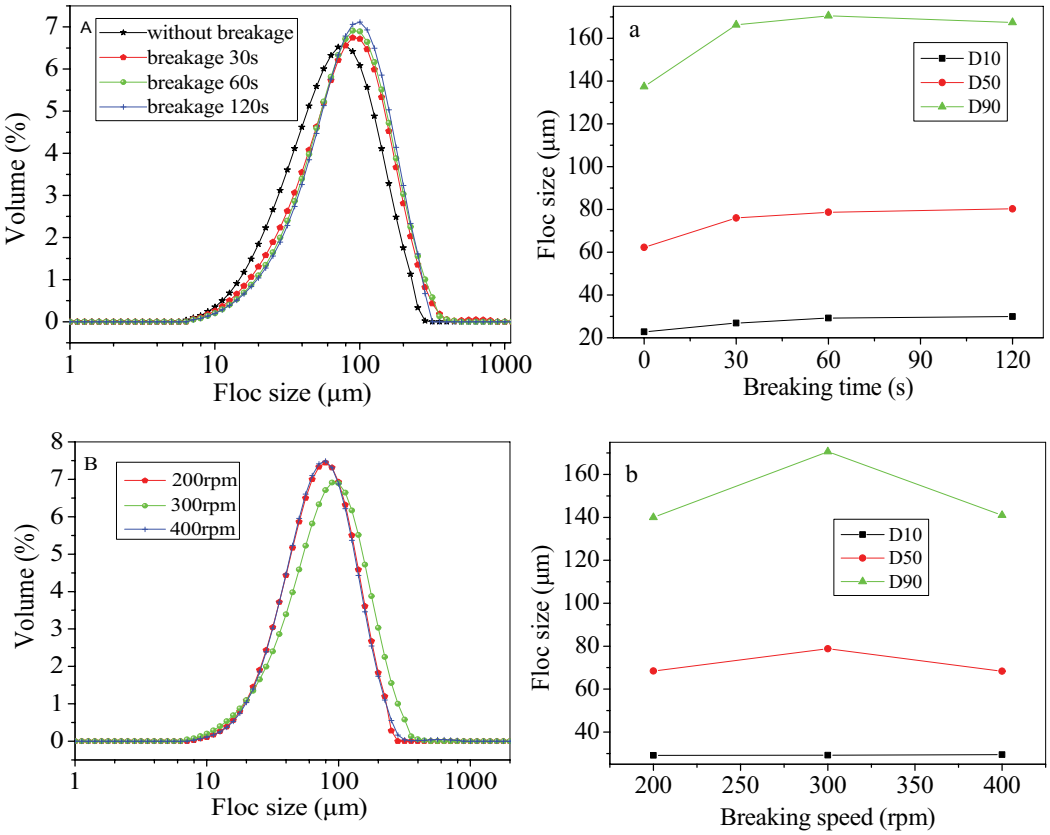

Fig. 3. Effects of breaking conditions on FSD (A) FSD of breaking time, (a) cumulative data of breaking time, (B) FSD of breaking speed, (b) cumulative data of breaking speed.

Table 1
Relationship between breaking speed and G value

Breaking speed (rpm)	G value (s^{-1})
200	93.6
300	161.5
400	243.9

analyzer. According to Fig. 5, the particle size of floc is relatively small due to the lack of adding PAM in the rapid stirring stage. During the period of 45 s and 90 s, D50 was 5.16 and 5.37 μm respectively, it can be seen that magnesium hydroxide- reactive orange floc is relatively small. There is no more aggregation occurred due to the strong repulsion between positively charged particles of magnesium hydroxide. The resulting repulsive forces tend to stabilize the suspension and prevent particle agglomeration.

After the use of PAM in the slow stirring phase, average floc size D50 increased to 43.20 μm at 150 s. It can be seen that the average particle size of floc can make a qualitative leap by only giving a short slow stirring time. Then, with the extension of slow stirring time, the average particle size of floc gradually increases, it reaches 62.29 μm at 270 s, compared with the previous fast stirring stage, it can fully prove that PAM has an excellent optimization effect on this experiment. In the breaking stage, the average particle size decreased again from 48.70 to 52.58 μm. During the re-growth stage (390–510 s) of slow stirring, the average particle size of floc increased from 60.77 to 78.75 μm. It can be seen that appropriate re-growth after breakage can make floc grow to a larger level. According to the trend lines of D10 and D90 in Fig. 5, the change of small particle floc is not obvious during the experiment, but its size is gradually increasing, while the change of large particle floc is obvious, and the trend is the same as that of D50.

The zeta potential decreased with increasing coagulation time in the early stage without breakage. During the break-up process under higher mixing conditions at 270 s, the flocs were broken into many smaller flocs and led to higher zeta potential –21.1 mV. This value is between –18.6 and –24.1 mV in coagulation process at 90 and 150 s. The break-up flocs may have different physical properties [23]. In re-growth period, zeta potential remains relatively stable at –27 mV. Prolong coagulation time cause zeta potential increase again. In the current study, charge neutralization was not sufficient to describe the phenomena observed. Magnesium hydroxide adsorption and PAM bridge function can be the main coagulation mechanisms. In practical case it is not easy to distinguish between the charge neutralization and adsorption process. Electrical charge or

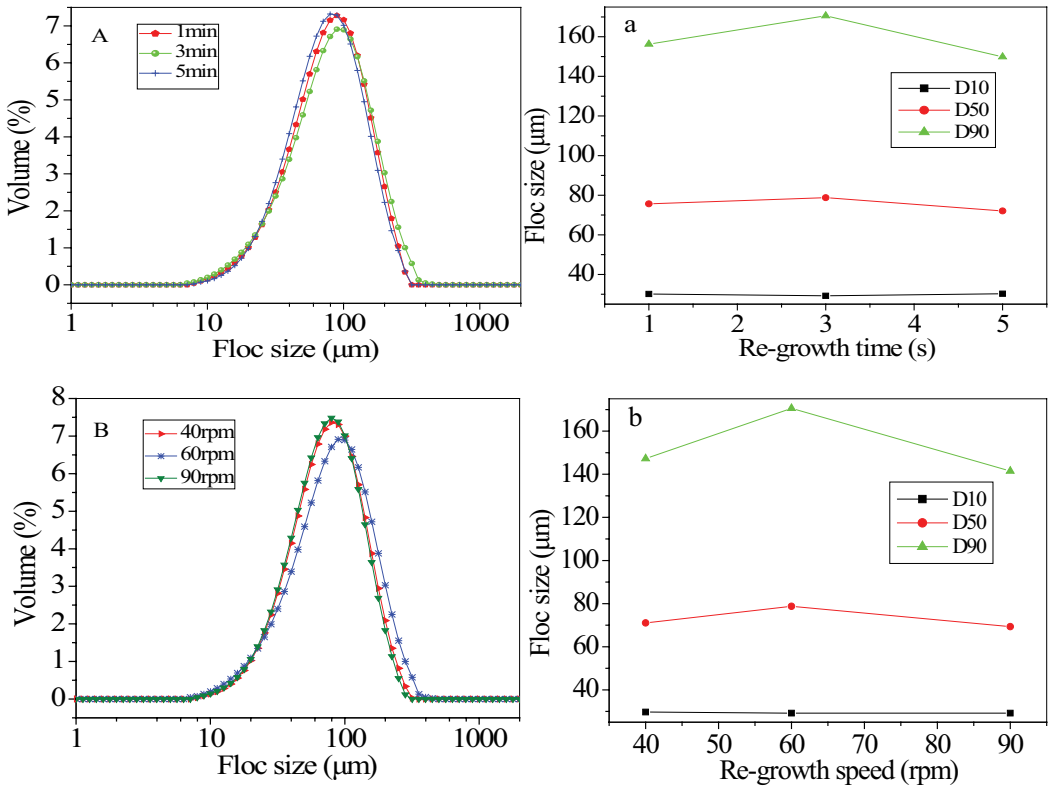

Fig. 4. Effects of re-growth conditions on FSD (A) FSD of re-growth time, (a) cumulative data of re-growth time, (B) FSD of re-growth speed, (b) cumulative data of re-growth speed.

Table 2
Relationship between re-growth speed and G value

Re-growth speed (rpm)	G value (s^{-1})
40	10.3
60	18.5
90	31.6

colloidal properties of the magnesium hydroxide-reactive dye flocs would be greatly affected. PAM promotes larger and tougher floc by a bridging function.

3.4. Floc and sediments characteristics

3.4.1. Floc image and XRD analysis

To ascertain further insight into floc and sediments properties, floc images were analyzed and the crystallographic structure was determined by X-ray diffraction. Samples of floc and sediments were withdrawn after sedimentation. The XRD patterns of the floc and sediments are presented in Fig. 6. The results of XRD proved the diffraction peaks were almost the same with and without breakage processes. Both of them indicated the presence of a crystalline structure evidenced by the appearance of peaks at 19°, 38° and 51°. Fig. 6 indicates that magnesium hydroxide crystal was obtained which is in good agreement with the standard pattern (JCPDS07-0239). Magnesium hydroxide has a positive superficial charge, which attracts the negatively charged reactive orange in coagulation process [24]. Fig. 7 clearly indicates that flocs aggregated together to form cotton-shape images with and without breakage. Although aggregates did not change significantly through breakage and re-growth, floc strength was different. After breakage and re-growth, flocs (shown in Fig. 7b) were more compact compared relatively loose flocs without breakage (Fig. 7a). PAM chain adsorbs on scatter magnesium hydroxide- reactive orange flocs and forms specific bridge between them. Magnesium hydroxide with bigger specific surface attracts negatively charged reactive orange and PAM accelerates the sedimentation rate of flocs [25].

3.4.2. Fourier-transform infrared spectral analysis and SEM

Fourier-transform infrared spectra of flocs and sediments with and without breakage are shown in Fig. 8. In analyzing these spectra of two processes, this information was then applied to the predicted different function of magnesium hydroxide, PAM and reactive orange. The stretching vibration frequency of hydroxyl functional groups generally appear at 3,400–3,700 cm^{-1}. The peak value of 3,700 cm^{-1} represents –OH, and the peak nearby is mainly caused by the free radical O–H stretching vibration [26]. Although NH is in similar region to OH, it looks very weak. These spectra indicate that for PAM. The peak of 1,610 cm^{-1} is due to bending vibration of Mg–OH, the emergence of peak 1,560 and 1,480 cm^{-1} is caused by the C=C double bond stretching vibration of

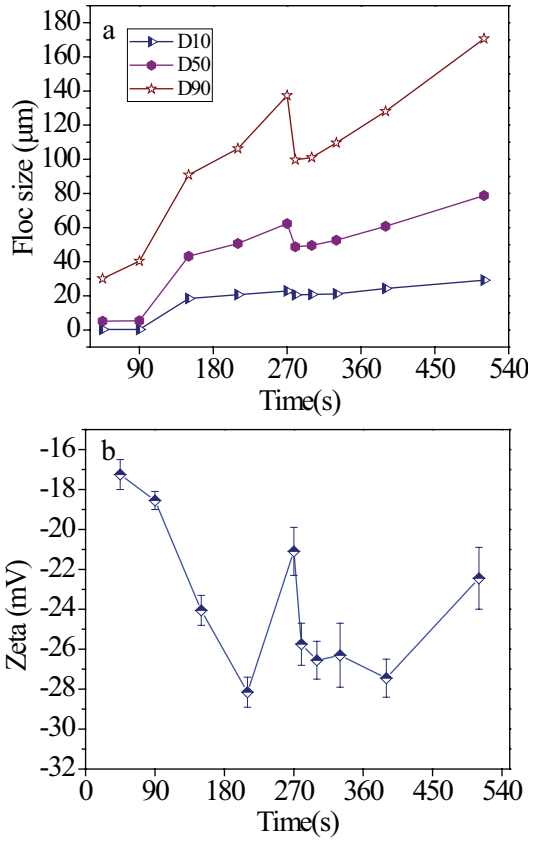

Fig. 5. Cumulative data of (a) FSD and (b) zeta potential.

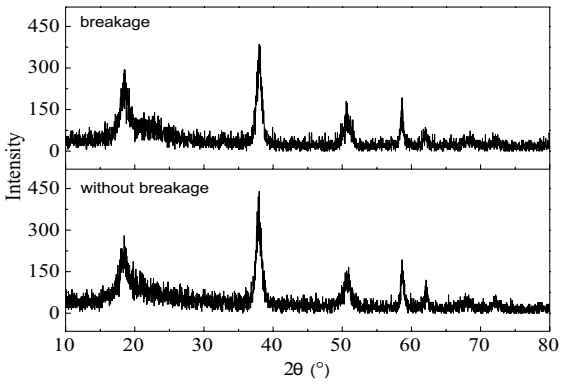

Fig. 6. XRD patterns of the sediments.

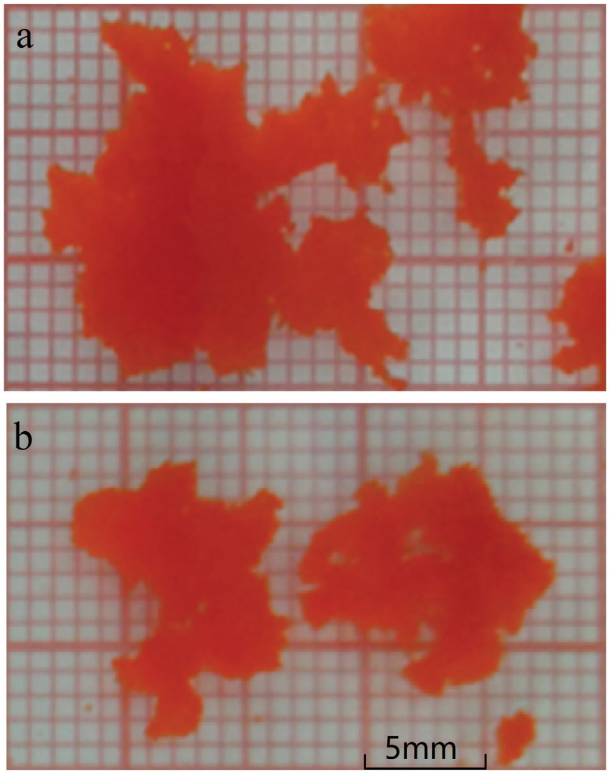

Fig. 7. Floc image analysis (a) without breakage and (b) breakage and re-growth.

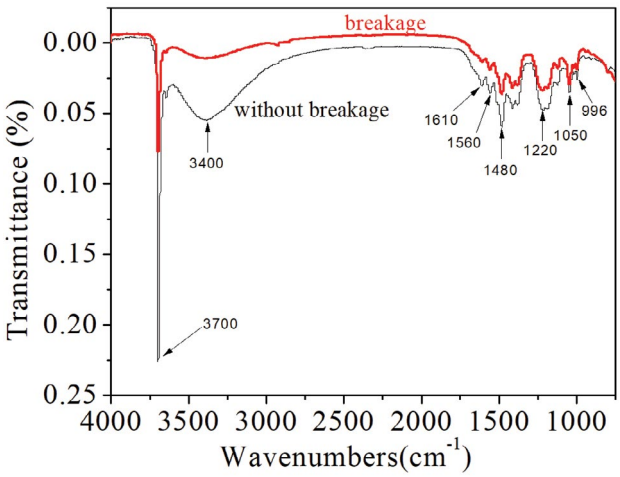

Fig. 8. Infrared spectra of coagulation flocs.

benzene ring in reactive dye, The peak value of 1,050 cm^{-1} is caused by the stretching vibration of alcohol C–OH.

In summary, the peaks of 3,700; 1,610 and 1,420 cm^{-1} in the infrared spectrum indicate that the product is magnesium hydroxide. Reactive orange K-GN is adsorbed on the surface of magnesium hydroxide during coagulation process. Breakage and re-growth caused floc size and sedimentation time changes rather than the original characteristics of materials.

The surface and morphology of flocs and sediments with and without breakage by scanning electron microscopy (SEM) images are illustrated in Fig. 9. There have significant changes in the surface morphology of dye-loaded sediments. According to the SEM image analysis, the flocs before breaking present irregular agglomeration and package shape, which indicate that PAM bridging plays a significant role in dual-coagulant system. The flocs after breakage and regeneration present irregular fish scales and irregular agglomeration and envelopment, suggesting that fragmentation and regeneration have reshaped the basic structure of flocs [27]. Reactive orange K-GN removal was mainly

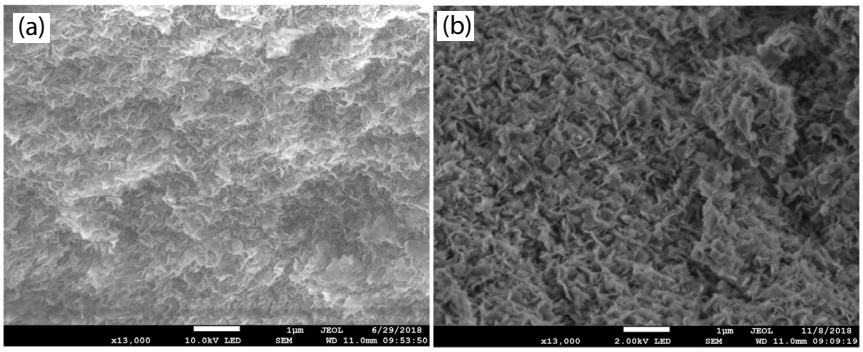

Fig. 9. SEM images of flocs (a) without breakage and (b) breakage and re-growth.

adsorbed by magnesium hydroxide and flocs aggregation depended on PAM bridging function.

4. Conclusions

- The study indicates that the removal efficiency with and without breakage is the same at 99.3% and there is only sedimentation time different which is reduced to 40 s (with breakage) from 60 s (without breakage).
- A significant drop first and then re-growth in FSD, as a result of floc breakage and aggregation, can be observed immediately when rapid break-up period and slow mixing steady state. A greater mixing intensity and time significantly affected breakage and re-growth processes.
- The optimum mixing conditions for flocs re-growth were obtained after normal coagulation process. The breakage and re-growth conditions were 300 rpm at 60 s and 60 rpm at 3 min, respectively.
- During the breakage and re-growth processes, larger flocs break into small particles, and then flocs aggregate again depending on PAM bridging function. All of the flocs under investigation showed a strong capacity to re-growth when they had been previously broken.

Acknowledgement

This work is supported by the National Key Research and Development Program of China (No. 2019YFE0122400).

References

[1] B.-Y. Gao, Q.-Y. Yue, Y. Wang, W.-Z. Zhou, Color removal from dye-containing wastewater by magnesium chloride, J. Environ. Manage., 82 (2007) 167–172.
[2] X. Huang, T. Wu, Y. Li, D. Sun, G. Zhang, Y. Wang, G. Wang, M. Zhang, Removal of petroleum sulfonate from aqueous solutions using freshly generated magnesium hydroxide, J. Hazard. Mater., 219–220 (2012) 82–88.
[3] H. Li, S. Liu, J. Zhao, N. Feng, Removal of reactive dyes from wastewater assisted with kaolin clay by magnesium hydroxide coagulation process, Colloids Surf., A, 494 (2016) 222–227.
[4] L. Semerjian, G.M. Ayoub, High-pH–magnesium coagulation–flocculation in wastewater treatment, Adv. Environ. Res., 7 (2003) 389–403.
[5] A.K. Verma, R.R. Dash, P. Bhunia, A review on chemical coagulation/flocculation technologies for removal of colour from textile wastewaters, J. Environ. Manage., 93 (2012) 154–168.
[6] J. Leentvaar, M. Rebhun, Effect of magnesium and calcium precipitation on coagulation–flocculation with lime, Water Res., 16 (1982) 655–662.
[7] A.Z. Bouyakoub, B.S. Lartiges, R. Ouhib, S. Kacha, A.G. El Samrani, J. Ghanbaja, O. Barres, $MnCl_2$ and $MgCl_2$ for the removal of reactive dye Levafix Brilliant Blue EBRA from synthetic textile wastewaters: an adsorption/aggregation mechanism, J. Hazard. Mater., 187 (2011) 264–273.
[8] J. Zhao, H. Shi, M. Liu, J. Lu, W. Li, Coagulation–adsorption of reactive orange from aqueous solution by freshly formed magnesium hydroxide: mixing time and mechanistic study, Water Sci. Technol., 75 (2017) 1776–1783.
[9] M. Liu, J. Lu, L. Wei, K. Wang, J. Zhao, Magnesium hydroxide coagulation performance and floc properties in treating high pH reactive orange wastewater, Water Sci. Technol., 71 (2015) 1310–1316.
[10] M. Lapointe, B. Barbeau, Dual starch-polyacrylamide polymer system for improved flocculation, Water Res., 124 (2017) 202–209.
[11] H. Liu, X. Yang, Y. Zhang, H. Zhu, J. Yao, Flocculation characteristics of polyacrylamide grafted cellulose from *Phyllostachys heterocycla*: an efficient and eco-friendly flocculant, Water Res., 59 (2014) 165–174.
[12] M. Wu, W. Yu, J. Qu, J. Gregory, The variation of flocs activity during floc breakage and aging, adsorbing phosphate, humic acid and clay particles, Water Res., 155 (2019) 131–141.
[13] M.I. Aguilar, J. Saez, M. Llorens, A. Soler, J.F. Ortuno, V. Meseguer, A. Fuentes, Improvement of coagulation–flocculation process using anionic polyacrylamide as coagulant aid, Chemosphere, 58 (2005) 47–56.
[14] A. Vahedi, B. Gorczyca, Application of fractal dimensions to study the structure of flocs formed in lime softening process, Water Res., 45 (2011) 545–556.
[15] J. Nan, Z. Wang, M. Yao, Y. Yang, X. Zhang, Characterization of re-grown floc size and structure: effect of mixing conditions during floc growth, breakage and re-growth process, Environ. Sci. Pollut. Res., 23 (2016) 23750–23757.
[16] Z. Wang, J. Nan, M. Yao, Y. Yang, Effect of additional polyaluminum chloride and polyacrylamide on the evolution of floc characteristics during floc breakage and re-growth process, Sep. Purif. Technol., 173 (2017) 144–150.
[17] G.M. Ayoub, S.W. BinAhmed, M. Al-Hindi, F. Azizi, Coagulation of highly turbid suspensions using magnesium hydroxide: effects of slow mixing conditions, Environ. Sci. Pollut. Res., 21 (2014) 10502–10513.
[18] W.Z. Yu, J. Gregory, L. Campos, G. Li, The role of mixing conditions on floc growth, breakage and re-growth, Chem. Eng. J., 171 (2011) 425–430.
[19] T. Li, Z. Zhu, D.S. Wang, Characterization of floc size, strength and structure under various coagulation mechanisms, Powder Technol., 168 (2006) 104–110.
[20] M. Rossini, J.G. Garrido, M. Galluzzo, Optimization of the coagulation–flocculation treatment: influence of rapid mix parameters, Water Res., 33 (1999) 1817–1826.

[21] X. Zhan, B.Y. Gao, Y. Wang, Q.Y. Yue, Influence of velocity gradient on aluminum and iron floc property for NOM removal from low organic matter surface water by coagulation, Chem. Eng. J., 166 (2011) 116–121.
[22] J. Colomer, F. Peters, C. Marrasé, Experimental analysis of coagulation of particles under low-shear flow, Water Res., 39 (2005) 2994–3000.
[23] E.L. Sharp, P. Jarvis, S.A. Parsons, B. Jefferson, The impact of zeta potential on the physical properties of ferric-NOM flocs, Environ. Sci. Technol., 40 (206) 3934–3940.
[24] G.M. Ayoub, F. Merhebi, A. Acra, M. El-Fadel, B. Koopman, Seawater bittern for the treatment of alkalized industrial effluents, Water Res., 34 (2000) 640–656.
[25] J. Zhao, B. Li, A. Wang, W. Ge, W. Li, Floc formation and growth mechanism during magnesium hydroxide and polyacrylamide coagulation process for reactive orange removal, Environ. Technol., 43 (2022) 424–430.
[26] H. Yan, X. Du, M. Zhang, J. Zhang, S. Ma, B. Xu, Synthesis and characterization of novel organic magnesium salt flame retardant, Mater. Lett., 134 (2014) 210–213.
[27] M. Yao, J. Nan, T. Chen, D. Zhan, Q. Li, Z. Wang, H. Li, Influence of flocs breakage process on membrane fouling in coagulation/ultrafiltration process – effect of additional coagulant of poly-aluminum chloride and polyacrylamide, J. Membr. Sci., 491 (2015) 63–72.